

## Binding of Ubiquinone to Photosynthetic Reaction Centers. 2. Determination of Enthalpy and Entropy Changes for the Binding to the Q<sub>A</sub> Site in Reverse Micelles

Antonia Mallardi<sup>†</sup> and Mauro Giustini<sup>‡</sup>

CNR, Centro Studi Chimico-Fisici sull'Interazione Luce-Materia, via Orabona 4, I-70126 Bari, Italy

Gerardo Palazzo\*

Dipartimento di Chimica, Università di Bari, via Orabona 4, I-70126 Bari, Italy

Received: June 3, 1998; In Final Form: August 31, 1998

The Q<sub>A</sub> site binding properties of the purple non-sulfur bacterium *Rhodobacter sphaeroides* reaction centers solubilized in phospholipid-based reverse micelles have been determined. By means of time-resolved absorbance measurements, the binding of the ubiquinone-10 to the Q<sub>A</sub> site has been followed at different temperatures and quinone concentrations yielding the relative binding constants. A global fit of the experimental data allowed us to get quite reliable values of the thermodynamic parameters joined to the binding process. Enthalpy and entropy changes obtained for the binding at the Q<sub>A</sub> site ( $\Delta H^\circ_{\text{bind}} = -75.3 \pm 3.4 \text{ kJ mol}^{-1}$  and  $\Delta S^\circ_{\text{bind}} = -181 \pm 11 \text{ J mol}^{-1} \text{ K}^{-1}$ ) confirm that the quinone binding to the primary site is stronger with respect to that at the Q<sub>B</sub> site. A Monte Carlo simulation of both the classical Van't Hoff and global analysis approaches is also presented, showing the higher reliability of the thermodynamic parameters derived with the latter method (uncertainty less than 1% with respect to more than 40% of the Van't Hoff analysis). Such an analysis indicates also that the enthalpy–entropy compensation previously observed through the ubiquinone series is likely due to a statistical artifacts.

### Introduction

In the photosynthetic membranes of purple bacteria, the reaction center (RC) protein complex catalyzes the conversion of light into electrochemical potential energy through a vectorial sequence of electron-transfer reactions starting from a bacteriochlorophyll dimer (the primary donor, P) to several redox cofactors, including quinones, that are held at fixed distances by the polypeptide scaffolding.<sup>1</sup>

In the RC two quinone molecules are bound to two different redox catalytic sites (Q<sub>A</sub> and Q<sub>B</sub>), which display distinct equilibrium binding properties.

In vivo the Q<sub>A</sub> site quinone, located in a hydrophobic pocket of the protein, acts as an apparently nonexchangeable cofactor. It is reduced to the anionic semiquinone (Q<sub>A</sub><sup>•−</sup>) in the light-driven electron-transfer sequence within the RC protein complex and, in turn, reduces a second quinone molecule bound at the Q<sub>B</sub> site, which is in a relatively polar protein domain.<sup>2</sup>

Unlike the Q<sub>A</sub> site quinone, the quinone bound at the Q<sub>B</sub> site, after the absorption of a second photon, is capable of accepting a second electron (again from Q<sub>A</sub><sup>•−</sup>) and, after the binding of two protons to form the hydroquinone species, it rapidly exchanges with a pool of quinone molecules localized in the hydrophobic core of the membrane bilayer.<sup>1,2</sup>

The physical–chemical factors that rule the light-induced electron-transfer reactions have been the subject of intense experimental scrutiny<sup>3</sup> and have stimulated the development of numerous theoretical descriptions.<sup>4</sup> On the contrary, systematic physical–chemical studies on the interaction among quinones

and RC protein complex at Q<sub>A</sub> and Q<sub>B</sub> sites have been invalidated by the extreme hydrophobicity of both the protein and the native quinone, which has limited the study of their interactions to microheterogeneous aqueous surfactant systems, characterized by topologically disconnected lipophilic domains dispersed in a continuous aqueous bulk, where both the kinetics and the equilibria of the quinone binding processes are strongly influenced by the structure and dynamics of the surfactant aggregates.<sup>5,6</sup>

Understanding the factors ruling the different quinone binding equilibria to these redox catalytic sites of the RC is a crucial point to obtain a complete comprehension of the mechanisms regulating the efficient capture and stable storage of free energy in photosynthesis.

The RC from *Rhodobacter sphaeroides*, which binds ubiquinone-10 (Q) to both Q<sub>A</sub> and Q<sub>B</sub> sites, has been solubilized in reverse micelles of phospholipids in *n*-hexane.<sup>7</sup> The exchange dynamic of the quinone to the Q<sub>B</sub> site has been successfully studied by us in this system, where the strong hydrophobic effects are absent and the influence of the micellar dynamics is negligible.<sup>8,9</sup> Moreover, the use of global analysis allowed an accurate determination of both the enthalpy and entropy changes associated with the quinone binding to the Q<sub>B</sub> site.

In the present study we extend the determination of the thermodynamic parameters to the binding of the native quinone at the Q<sub>A</sub> site of the RC of *Rb. sphaeroides* solubilized in phospholipid-based reverse micelles. The quinone binding was followed at several temperatures, and the results were analyzed by means of global analysis, in order to obtain more reliable values of the enthalpy and entropy changes associated to this process. The Monte Carlo analysis, performed on the values obtained from this procedure, confirms the effectiveness of our

\* To whom correspondence should be addressed. E-mail: palazzo@area.ba.cnr.it.

<sup>†</sup> E-mail: mallardi@area.ba.cnr.it.

<sup>‡</sup> E-mail: giustini@area.ba.cnr.it.

experimental data treatment with respect to those reported in the literature.

## Materials and Methods

**Chemicals.** Ubiquinone-10, phosphatidylserine (brain extract, type III: folch fraction III from bovine brain), and phosphatidylethanolamine (type II-S: from sheep brain) were from Sigma and used without further purification. Soybean phosphatidylcholine (Epikuron 200) was a generous gift from Lucas-Meyer GmbH. Sephadex G-50 was purchased from Pharmacia, while *n*-Hexane (for UV spectroscopy) was from Fluka.

**Preparation of RC-Containing Reverse Micelles.** RCs from *Rb. sphaeroides* were isolated and purified as already described.<sup>10</sup>

In all the preparations the ratio between the absorption at 280 nm and the absorption at 800 nm was about 1.2. The concentration of the RC was determined spectrophotometrically by the absorbance at 802 nm ( $\epsilon = 288 \text{ mM}^{-1} \text{ cm}^{-1}$ ).

Quinone-depleted RCs were prepared according to the method of Okamura et al.<sup>11</sup> Approximately 80% of the RCs had been depleted of quinone, as judged from measurements of the reduced amplitude of the absorbance changes at 600 nm, after excitation with a short flash, indicative of the decrease in the formation of the charge-separated state (because of the  $Q_A$  depletion).

Typically,  $5 \times 10^{-9}$  mol of Q-depleted RCs were added to a phospholipid mixture made of phosphatidylserine (PS), phosphatidylethanolamine (PE), and phosphatidylcholine (PC), at a mole ratio of 2:1:1, previously dispersed in 10 mM imidazole, 100 mM KCl, and 3% Na-cholate buffer (pH = 7) and sonicated (Branson Sonifier 250) on ice until a transparent solution was obtained. The molar ratio [total lipids]/[RC] was 4500. The final mixture was applied onto a column ( $1 \times 10$  cm) of Sephadex G-50 equilibrated in 10 mM imidazole, 100 mM KCl buffer, pH = 7, and eluted with the same buffer at room temperature. The reconstituted proteoliposomes were extracted with 1.5 mL of *n*-hexane after addition of 100  $\mu\text{L}$  of 1 M  $\text{MgCl}_2$ , according to Mallardi et al.<sup>8</sup>

For the reconstitution of the  $Q_A$  functionality, to the reverse micellar solution of the Q-depleted RCs, different amounts of quinone (as *n*-hexane solution) were added up to the desired final Q concentration.<sup>12</sup>

**Spectroscopic Measurements.** The reconstitution (binding) of ubiquinone-10 (Q) to the  $Q_A$  site was deduced by the increment in the net amplitude of the absorbance changes at 600 nm following a single turnover flash experiment.

After a flash, when Q is bound to the protein a decrease of the absorption at 600 nm, indicative of a charge separation between  $\text{P}^+\text{Q}_A^-$  (or  $\text{P}^+\text{Q}_B^-$ , depending on Q concentration), is observed. The  $\text{P}^+$  dark re-reduction was fitted to a single or to a double exponential (according to the Q concentration), and the extent of the bleaching at time 0 ( $\Delta\text{Abs}^\circ_{600}$ ) was taken as a quantity directly related to the reconstitution.

Single turnover flash experiments were performed using an Optical Multichannel Analyzer (EG&G, OMA III, model 1460) equipped with an EG&G Red Intensified Diode Array Detector model 1420-512-G. Actinic flashes were provided by two xenon lamps (3.25 J discharge energy each, EG&G), both mounted at a right angle from the measuring beam, giving a subsaturating 4  $\mu\text{s}$  wide light pulse (at its half-maximal intensity). Flash synchronization was provided by a TTL pulse originating from the OMA III and reaching the flash discharge units through a home-built delay unit. Temperature was

measured by a Pt100 ceramic resistor probe (DEGUSSA, tolerance  $\pm 0.3^\circ\text{C}$ ) inserted into the cuvette (1 cm path length, HELIMA QS-282). The temperature was kept constant by a HAAKE thermocryostat (model DC3-K20). For the measurements at fixed quinone concentration and variable temperature, a waiting period of at least 15 min (starting from the moment the temperature reached the desired value) occurred before starting the acquisition.

**Data Analysis.** The sequential analysis and the simultaneous global analysis described in the text were performed by using the "STEFIT" software (STELAR s.n.c.). The error estimation of the parameters obtained by the fits was performed by means of Monte Carlo simulation with the same software, using the appropriate macro program. The overall approach was as follows. The parameters obtained by fitting the set of experimental data to the appropriate function were used to create "perfect" data sets applying the chosen equation. Random noise, corresponding to the standard deviation obtained by the best fit of the experimental data, was added to the perfect data set. The data were then fitted by a least-squares routine (using the SIMPLEX algorithm) to the selected model. This process was repeated 1000 times, taking care to add a different set of noise to the perfect data before each cycle. The best fit parameters were analyzed for the mean and standard deviation.

## Results

In reverse micelles, the RCs lack any exogenous electron donor to  $\text{P}^+$  and the charge recombination between the flash-generated species is observed. When quinone-depleted RCs are solubilized in micellar solution, the charge separation is limited to the bacteriopheophytin molecule (the intermediate electron acceptor) and the subsequent charge recombination occurs on a time scale shorter than the flash width.<sup>1</sup> Therefore, it is not possible to detect any absorbance change. In the presence of a pool of quinone molecules dissolved in the continuous organic phase, the binding sites of the protein are occupied by quinones according to

$$[\text{RCQ}_i] = \frac{[\text{RC}]_{\text{tot}}[\text{Q}]_f}{K_{\text{D},Q_i} + [\text{Q}]_f} \quad (1)$$

where  $[\text{RCQ}_i]$  indicates the protein concentration with the  $Q_i$  site occupied,  $K_{\text{D},Q_i}$  is the dissociation constant for the  $i$  site, and  $[\text{Q}]_f$  denotes the free quinone concentration. Since both the  $Q_A^-$  and the  $Q_B^-$  states are long-lived compared to the flash width, it is possible to follow the time course of the charge recombination.<sup>1</sup> Furthermore, since the photoinduced electron transfer up to  $Q_B$  is possible only through  $Q_A$ , the proteins with the  $Q_B$  site occupied and the  $Q_A$  site empty do not contribute to the observed signal. The time course of the charge recombination process has been previously investigated in reverse micelles. It is characterized by a single-exponential decay for the  $\text{P}^+\text{Q}_A^- \rightarrow \text{PQ}_A$  process and by a two-exponential decay for a RC population containing a protein fraction with  $Q_B$  site reconstituted (further details have been reported elsewhere<sup>8</sup>). The decay of  $\text{P}^+$  following a light flash was monitored at 600 nm at different quinone concentrations ( $[\text{Q}]$ ) and temperatures. The experimental traces were fitted to one or two exponentials (depending on their features), thus obtaining the amplitude of the bleaching at time  $t = 0$ . Such a quantity is proportional to the concentration of RC with the  $Q_A$  site occupied according to

$$\Delta\text{Abs}^\circ_{600} = F[\text{RCQ}_A] \quad (2)$$

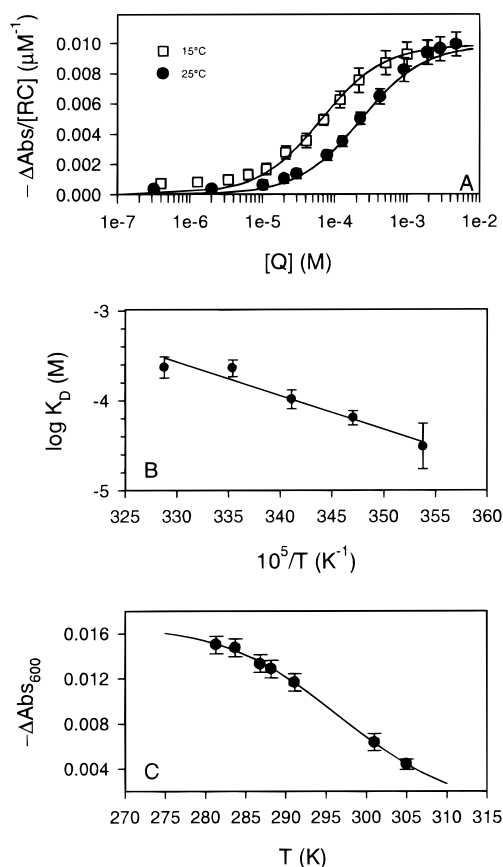


**Figure 1.**  $\text{Q}_\text{A}$  site functionality reconstitution for RCs solubilized in phospholipid reverse micelles. (A) Titration curves of the  $\text{Q}_\text{A}$  site occupancy as a function of the ubiquinone-10 concentration at two different temperatures. The experimental absorbances have been normalized for the RC concentration. The continuous lines are the best fits according to eqs 2 and 3. The binding constants at 15 and 25 °C are, respectively,  $4.85 \times 10^{-5}$  and  $2.08 \times 10^{-4}$  M. (B) Van't Hoff plot of the  $K_D$  values obtained from the binding isotherms. The solid line is the best fit according to eq 4. (C) Dependence of the bleaching at 600 nm on the temperature ( $[\text{RC}] = 1.86 \mu\text{M}$  and  $[\text{Q}] = 87.8 \mu\text{M}$ ). The solid line is the best fit according to eqs 2, 3, and 4.

where  $F$  depends on the differences in the molar absorptivities between  $\text{P}^+$  and  $\text{P}$  and on the degree of saturation of the light pulse (two typical titration curves are shown in Figure 1A). It should be stressed that the double-exponential behavior for the  $\text{P}^+$  decay starts to appear for  $\text{Q}$  concentration values 3–4 orders of magnitude greater than the stoichiometric RC concentration. This means that the contribution of the binding to the  $\text{Q}_\text{B}$  site can be neglected in the calculation of the  $[\text{Q}]_\text{f}$ . Accordingly, for an isothermal binding curve the following relationship holds:

$$[\text{RCQ}_\text{A}] = \frac{([\text{RC}]_\text{tot} - [\text{RCQ}_\text{A}])([\text{Q}] - [\text{RCQ}_\text{A}])}{K_{\text{D,AQ}}} \quad (3)$$

Thus, it is possible to fit the experimental values of each binding isotherms to eqs 2 and 3 with  $F$  and  $K_{\text{D,QA}}$  as the only adjustable parameters. Such a “sequential” analysis,<sup>13</sup> results in a larger uncertainty in the obtained parameters when compared to the global analysis approach described below. However, although rough, such an approach allows some preliminary conclusions to be drawn. First, eqs 2 and 3 describe satisfactorily (continuous lines in Figure 1A) the experimental behavior, and most important, the dissociation constants obtained are (at all the investigated temperatures) 10-fold smaller than the dissociation constants for the  $\text{Q}_\text{B}$  site (previously determined by us<sup>8</sup>). These

features confirm that it is correct to neglect the fraction of quinone bound to the  $\text{Q}_\text{B}$  site. An accurate inspection of Figure 1A shows a systematic deviation from the prediction at low  $[\text{Q}]$ ; such deviations are greater at low temperatures. This arises from the difficulty in evaluating the amount of  $\text{Q}$  extracted into *n*-hexane (the fraction of protein and quinone extracted from liposomes are likely different). This is the reason our analysis was limited to the data obtained with an excess of quinone ( $[\text{Q}] > 10^{-5}$  M).

The temperature influence on the binding equilibrium is still described by eq 3 once the temperature dependence of the dissociation constant is taken into account:

$$K_{\text{D,QA}} = \exp\left(\frac{\Delta H^\circ_{\text{bind}}}{RT} - \frac{\Delta S^\circ_{\text{bind}}}{R}\right) \quad (4)$$

where  $R$  is the gas constant,  $T$  is the thermodynamic temperature, and  $\Delta H^\circ_{\text{bind}}$  and  $\Delta S^\circ_{\text{bind}}$  are the enthalpy and entropy changes associated to the  $\text{Q}$  binding. In eq 4 both  $\Delta H^\circ_{\text{bind}}$  and  $\Delta S^\circ_{\text{bind}}$  are, in principle, functions of the temperature. The Van't Hoff plot of Figure 1B does not show any evident deviation from the linearity and can be accurately fitted by a straight line, giving guess parameters  $\Delta H^\circ_{\text{bind}} = -67 \text{ kJ mol}^{-1}$  and  $\Delta S^\circ_{\text{bind}} = -154 \text{ J mol}^{-1} \text{ K}^{-1}$ . These results are only indicative and should be taken with caution. In fact, there is a strong statistical correlation between  $\Delta H^\circ_{\text{bind}}$  and  $\Delta S^\circ_{\text{bind}}$  in eq 4,<sup>14</sup> resulting in a large uncertainty affecting both the parameters (the standard deviations evaluated by Monte Carlo analysis are  $9 \text{ kJ mol}^{-1}$  and  $29 \text{ J mol}^{-1} \text{ K}^{-1}$  for  $\Delta H^\circ_{\text{bind}}$  and  $\Delta S^\circ_{\text{bind}}$ , respectively). Furthermore, small thermal capacity changes can induce negligible deviations from the linearity of the Van't Hoff plot but a systematic bias on its slope.<sup>15</sup> Measurements performed at a given (high)  $[\text{Q}]$  and different temperatures are nicely described by eqs 2, 3, and 4 as shown in Figure 1C (in this last case,  $[\text{Q}]$  is a fixed parameter and  $T$  is the independent variable). This last result confirms that the deviations present in the low-temperature binding isotherms, for  $[\text{Q}] < 10^{-5}$  M, are due to a bias on the quinone concentration and not to a temperature-induced structural modification of the protein or of the micellar system. Most important, Figure 1C is a further indication that the changes in thermal capacity are small (if there are any). Accordingly, in the following we will consider both  $\Delta H^\circ_{\text{bind}}$  and  $\Delta S^\circ_{\text{bind}}$  as temperature-independent. It should be stressed that the same assumption was previously made for the binding of quinone to the  $\text{Q}_\text{B}$  site in reverse micelles<sup>8</sup> and to the  $\text{Q}_\text{A}$  site in aqueous detergent solutions<sup>5</sup>, and thus do not preclude a comparison among these values. However, the  $\Delta H^\circ_{\text{bind}}$  and  $\Delta S^\circ_{\text{bind}}$  obtained in the  $T$ -variable experiment are sensibly different ( $-99 \text{ kJ mol}^{-1}$  and  $-254 \text{ J mol}^{-1} \text{ K}^{-1}$ , respectively) from those coming from a Van't Hoff analysis, highlighting the huge error associated with these analyses. To overcome, at least in part, this problem a global analysis of all the data set has been performed. That is, all the experimental data points coming from different binding isotherms and from variable temperature experiments were simultaneously fitted to eqs 2, 3, and 4 by means of a least-squares regression. In this procedure all the points with the same RC concentration share the same  $F$  value (since the degree of flash-saturation depends on  $[\text{RC}]$ ) and, obviously,  $\Delta H^\circ_{\text{bind}}$  and  $\Delta S^\circ_{\text{bind}}$  are the same for the full data set. As shown in Figure 2 the agreement between the experimental data and the best-fit values is good. The results are listed in Table 1 together with the value recently obtained by us for the binding to the  $\text{Q}_\text{B}$  site in reverse micelles.<sup>8</sup>



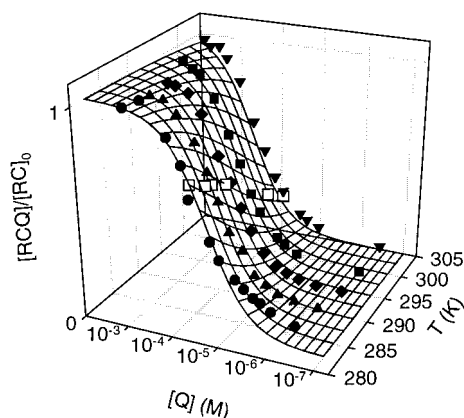


**Figure 2.** 3D-plot of the binding isotherms as a function of both the temperature and the quinone concentration. The surface is the best fit according to eqs 2, 3, and 4 obtained by the global analysis approach. Enthalpy and entropy changes are listed in Table 1 (see text for the details). Filled symbols, experiments performed at fixed temperature and variable Q concentration; hollow symbols, experiments performed at fixed Q concentration and variable temperature (same data as in Figure 1C).

**TABLE 1: Thermodynamical Parameters of Quinone Binding and of the Quinone Transfer from the Q<sub>B</sub> to the Q<sub>A</sub> Site<sup>a</sup>**

	Q <sub>A</sub> site <sup>b</sup>	Q <sub>B</sub> site <sup>c</sup>	Q <sub>B</sub> → Q <sub>A</sub>
$\Delta H^\circ$ (kJ mol <sup>-1</sup> )	$-75.3 \pm 3.4^e$	$-50.7 \pm 3.8^e$	$-24 \pm 7$
$\Delta S^\circ$ (J mol <sup>-1</sup> K <sup>-1</sup> )	$-181 \pm 11^e$	$-132 \pm 15^e$	$-49 \pm 26$
$\Delta G^\circ$ (kJ mol <sup>-1</sup> ) <sup>d</sup>	$-21.4 \pm 0.1^e$	$-11.4 \pm 0.9^e$	$-9.7 \pm 1$

<sup>a</sup> Values refer to molar standard state. <sup>b</sup> This work. <sup>c</sup> Reference 8. <sup>d</sup>  $T = 298$  K. <sup>e</sup> Standard deviation from MC simulation.

## Discussion

A first step in any discussion of the experimental results should be the evaluation of their accuracy and precision. A straightforward evaluation of the significance of the calculated values can be obtained by a Monte Carlo (MC) simulation.<sup>16,17</sup> The distribution of  $\Delta H^\circ_{\text{bind}}$  and  $\Delta S^\circ_{\text{bind}}$  obtained from both global and sequential (Van't Hoff) analysis of the data (1000 runs in each case) is shown in Figure 3, and it clearly illustrates the higher precision of the former approach. By means of MC simulation it is possible to properly take into account the correlation between  $\Delta H^\circ_{\text{bind}}$  and  $\Delta S^\circ_{\text{bind}}$  proper to the best fit procedure and evaluate  $\Delta G^\circ_{\text{bind}}$  at a given temperature, obtaining, in the case of global analysis, values characterized by extremely small uncertainties (less than 0.6%, see Figure 4A). The  $\Delta H^\circ_{\text{bind}}$  and the  $\Delta S^\circ_{\text{bind}}$  parameters are often highly correlated with each other. Such a correlation can be evaluated turning to the help of a correlation plot, in which the estimate for one parameter is plotted versus the other for all the simulated cases.<sup>17</sup> The cross-correlation coefficient is indicated by the distribution or randomness of the data. By making such a correlation analysis, one notices the high statistical correlation between  $\Delta H^\circ_{\text{bind}}$  and  $\Delta S^\circ_{\text{bind}}$  predicted by Krug et al.<sup>14</sup> In particular, the MC simulation of a Van't Hoff analysis results in a straight line for the  $\Delta H^\circ_{\text{bind}}$  vs  $\Delta S^\circ_{\text{bind}}$  plot, with a slope close to the mean harmonic temperature of the experiment (292.8 K in our case, see Figure 4B), and the same result is obtained from the global analysis (not shown). Such a feature can give insight into the enthalpy/entropy compensation phenomenon previously reported for the binding of the ubiquinone series to the Q<sub>A</sub> site in RC in water.<sup>5</sup> At this point it is interesting to compare our results to the enthalpy and entropy of binding determined in aqueous LDAO systems for ubiquin-

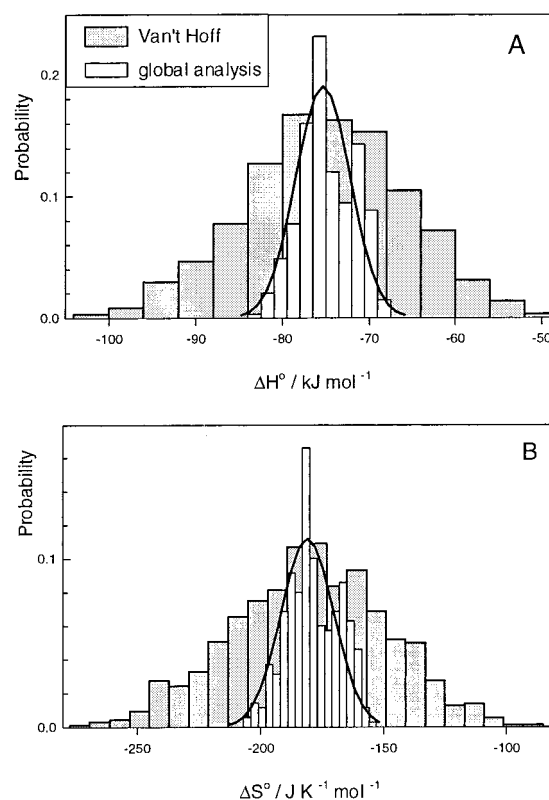


**Figure 3.** Distribution curves for  $\Delta H^\circ_{\text{bind}}$  (A) and  $\Delta S^\circ_{\text{bind}}$  (B), relative to both global (white) and Van't Hoff (gray) analysis of the experimental data, obtained by Monte Carlo simulations (1000 runs in each case, see text for the details). The solid lines are the Gaussian distributions built with the parameters of Table 1.

ones with different tail lengths.<sup>5</sup> In a correlation plot,  $\Delta H^\circ_{\text{bind}}$  vs  $\Delta S^\circ_{\text{bind}}$ , all the data lie on a straight line encompassing a wide  $\Delta H^\circ_{\text{bind}}$  and  $\Delta S^\circ_{\text{bind}}$  interval (from  $-79$  to  $15$  kJ mol<sup>-1</sup> and from  $-193$  to  $133$  J mol<sup>-1</sup> K<sup>-1</sup>, respectively, Figure 5A). This is quite surprising, and suspect as well, since the plot contains results coming from aqueous and nonaqueous systems where the contributions of the hydrophobic interaction are likely different. Actually, the slope of the line is 291.4, such a value being very close to the mean harmonic temperature,<sup>18</sup> and it suggests that the enthalpy/entropy compensation observed for the binding of the components of the ubiquinone series to the Q<sub>A</sub> site is merely a statistical artifact, and the correlation observed is a mathematical rather than a chemical correlation.<sup>14</sup> An additional and more convincing means of evaluating whether this is a real compensation or a statistical artifact is to plot enthalpy versus free energy at the mean harmonic temperature<sup>14</sup> as shown in Figure 5B. The uncorrelated behavior between  $\Delta H^\circ_{\text{bind}}$  and  $\Delta G^\circ_{\text{bind}}$  through the ubiquinone series indicates that there are not extrathermodynamical relationships between enthalpy/entropy changes for the quinone binding to the Q<sub>A</sub> site. Accordingly, the correlation between the extent (and the nature) of intermolecular forces (enthalpy term) and the amount of residual motion (entropy term) in the RC-Q complex is negligible. This offers the possibility of an easy, although somewhat rough, interpretation of the thermodynamical parameters of the quinone binding.

The change of a generic state function (Y) associated to the transfer of a quinone molecule from the Q<sub>B</sub> to the Q<sub>A</sub> binding site ( $\Delta Y^\circ_{\text{QB,QA}}$ ) can be easily evaluated from the thermodynamical cycle shown in Figure 6, where,  $\Delta Y^\circ_{\text{Q}}$ , denotes the change in Y associated with the binding of the quinone to the *i* site of the RC. The corresponding values of  $\Delta H^\circ$ ,  $\Delta S^\circ$ , and  $\Delta G^\circ$  are

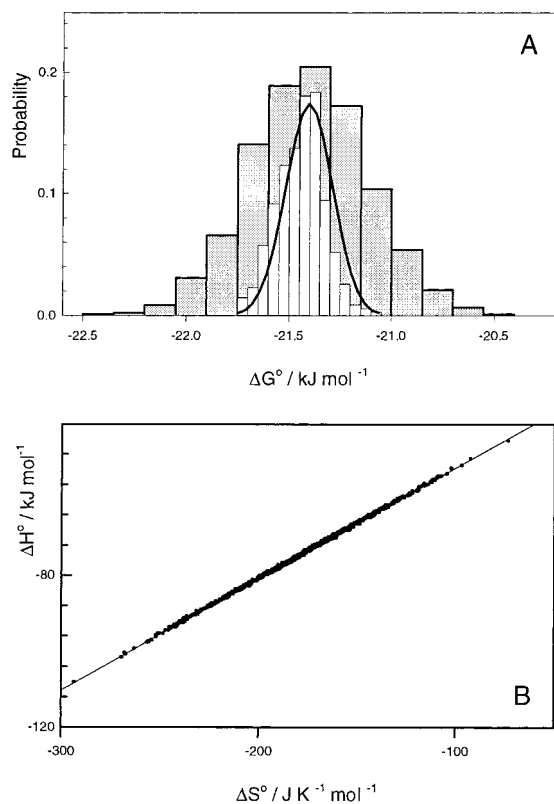


**Figure 4.** (A) Distribution curves for  $\Delta G^\circ_{\text{bind}}$  (at 298 K), relative to both global and Van't Hoff analysis of the experimental data, obtained by Monte Carlo simulations (1000 runs in each case, see text for the details). The solid line is the Gaussian distribution built with the parameters of Table 1. (B) Correlation plot  $\Delta H^\circ$  vs  $\Delta S^\circ$  obtained by Monte Carlo simulation of the Van't Hoff analysis (1000 runs); the slope is 292.9 K ( $r^2 = 0.9994$ ).

listed in Table 1. Such values are of considerable interest because they reflect the differences between the two binding sites in the quinone–protein interactions and in the degree of freedom of the two complexes as well. The greater affinity of the quinone for the  $Q_A$  site (negative value of  $\Delta G^\circ_{\text{QB},Q_A}$ ) can be conveniently analyzed in terms of enthalpic and entropic contributions. Since the transfer of quinone from  $Q_B$  to  $Q_A$  site is exothermic (negative value of  $\Delta H^\circ_{\text{QB},Q_A}$ ), it indicates an increase in the number and/or in the strength of the protein–quinone interactions. This is fully consistent with the present knowledge of the RC–quinone complex structure, based on crystallographic data. In the *Rb. sphaeroides* RCs, both the carbonyl oxygens of the quinone in the  $Q_A$  site form multiple close hydrogen bonds<sup>19,20</sup> whereas in the  $Q_B$  binding site only one of the carbonyl oxygens hydrogen bonds to the protein pocket.<sup>20,21</sup>

The interpretation of the  $\Delta S^\circ_{\text{QB},Q_A}$  is less straightforward. There is an entropic cost associated with any bimolecular interaction. This is a consequence of the loss of motional degrees of freedom when two molecules are rigidly constrained within a complex. The estimation of this cost is difficult for different reasons.<sup>22,23</sup> First of all, the entropy evaluation of the molecules in solution are subject to uncertainties. Second, the amount of residual motion present in a complex formed by an associative process in solution is also uncertain. However, working with  $\Delta S^\circ_{\text{QB},Q_A}$ , one removes the uncertainties associated with the entropy values of both the quinone and the (empty) protein in solution (the starting state is the same for the binding to both the sites  $Q_A$  and  $Q_B$ , see Figure 6). Accordingly, the decrease in entropy associated to the quinone transfer from  $Q_B$

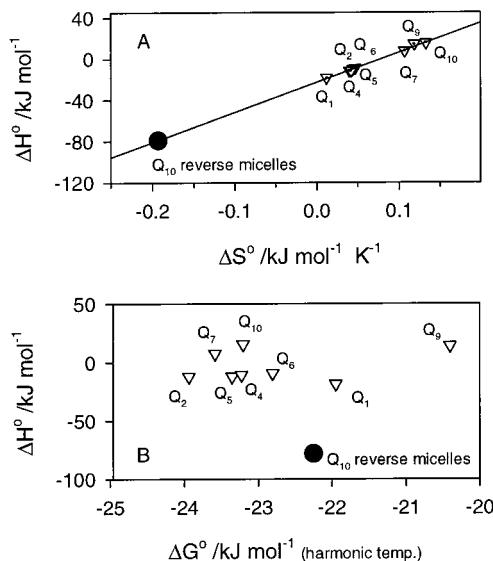


**Figure 5.** Correlation plots for aqueous LDAO and for phospholipid-based reverse micellar systems. (A)  $\Delta H^\circ_{\text{bind}}$  vs  $\Delta S^\circ_{\text{bind}}$  for the  $Q_A$  site. The white triangles refer to ubiquinones with different tail lengths in aqueous LDAO solutions (from ref 5), and the black circle refers to the data of Table 1 (the symbols' dimensions are of the same order of the uncertainty). The slope of the linear regression is 291.4 ( $r^2 = 0.9986$ ). (B)  $\Delta H^\circ_{\text{bind}}$  vs  $\Delta G^\circ_{\text{bind}}$  at the harmonic temperature (same symbols as in (A)). The harmonic temperature is 293 K for experiments in reverse micelles and 291 K for LDAO solutions. (The  $r^2$  in this case is extremely low,  $9.3 \times 10^{-4}$ .)

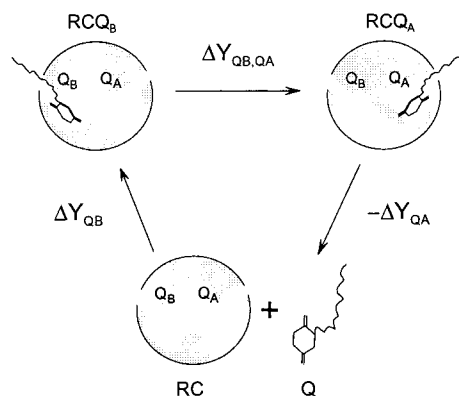


**Figure 6.** Pictorial representation of the proposed thermodynamic cycle that links quinone–protein binding equilibria for the  $Q_A$  and the  $Q_B$  sites through the transfer of a quinone molecule from the  $Q_B$  site to the  $Q_A$  site.  $Y$  represents a generic state function,  $\Delta Y_{Q_i}$  is the change in  $Y$  associated with the quinone binding to the  $Q_i$  site while  $\Delta Y_{\text{QB},Q_A}$  is the change in  $Y$  associated with the quinone translocation.

to  $Q_A$  ( $\Delta S^\circ_{\text{QB},Q_A} = -49 \text{ J K}^{-1} \text{mol}^{-1}$ , Table 1) is related to a decrease in the residual motion present in the complex (the sum of the translational and rotational entropies of the quinone–protein complex should be the same without regard to the quinone binding site). This is qualitatively in agreement with the idea of a quinone bound to a tight pocket in the protein structure forming the  $Q_A$  site and loosely bound to a flexible “hole” present in the protein structure accommodating the secondary quinone site ( $Q_B$ ).<sup>19–21</sup>

A final consideration about the absolute values of the binding entropy should be made. Although, as stated above, it is difficult to evaluate the correct values for the binding entropy, it is useful to compare the experimental values with the loss of translational and rotational entropies expected for ubiquinone upon binding. The loss in translational entropy can be easily evaluated<sup>24</sup> from the entropy in the gas phase taking into account the condensation

of the gas by means of Trouton's law and the dilution to a 1 M standard state, giving  $\Delta S_{\text{TRANS}} \approx -109 \text{ J K}^{-1} \text{ mol}^{-1}$ . The loss in the rotational entropy for a molecule of molecular weight of 863 is  $\Delta S_{\text{ROT}} \approx -(84 \div 115) \text{ J K}^{-1} \text{ mol}^{-1}$  according to ref 22. Thus  $\Delta S_{\text{TRANS}} + \Delta S_{\text{ROT}} = -(193 \div 224) \text{ J K}^{-1} \text{ mol}^{-1}$ .

Any loss in the internal degree of rotation of the molecule or of the protein (hindered motion of the rotors) will result in more negative  $\Delta S_{\text{bind}}$ , while the appearance of new vibrational motions in the complex will give a positive contribution to the experimental binding entropy. Actually, the value of  $\Delta S_{\text{TRANS}} + \Delta S_{\text{ROT}}$  is close to the experimental value of  $\Delta S_{\text{QA}}$ . Since we expect a partial freezing of the rotors of the first three isoprenic subunits upon binding<sup>9</sup> (with an expected decrease of about  $21 \text{ J K}^{-1} \text{ mol}^{-1}$  per rotor<sup>22,24</sup>), a further entropy-increasing process it is likely to happen. As stated above, low vibrational motions of the complex (absent in the dissociated state) can be responsible for the low  $|\Delta S_{\text{QA}}|$  value. The same explanation can be invoked for the binding to the  $Q_B$  site, which is characterized by a lower value of the binding-entropy decrease. However, the release of some water molecules can give a more straightforward explanation. Five water molecules, sharing the same volume of a quinone headgroup, have been found in the crystals of reaction centers from *Rhodospseudomonas viridis*,<sup>25</sup> thus supporting this idea. The  $Q_A$  site being more hydrophobic than the  $Q_B$  pocket, a lower occupancy of the first (empty) site by  $\text{H}_2\text{O}$  molecules it is likely. This is consistent with the  $|\Delta S_{\text{QB}}| < |\Delta S_{\text{QA}}|$  scale and with the decrease in binding constant (for the  $Q_B$  site) observed in aqueous solutions of high osmolarity<sup>26</sup> and in the organogels.<sup>27</sup>

## Conclusions

The binding enthalpy and entropy changes for the ubiquinone-10 to the  $Q_A$  site of bacterial reaction center (*Rb. sphaeroides* R-26 strain) in reverse micelles have been evaluated by global analysis of the occupancy of the binding site. Monte Carlo simulations clearly show that this approach is more precise than a sequential (Van't Hoff) analysis of the binding isotherms, indicating that there are not enthalpy/entropy compensation effects throughout the whole ubiquinone series. The comparison between  $\Delta H^\circ$  and  $\Delta S^\circ$  values for the binding to the  $Q_A$  and to the  $Q_B$  site is consistent with the protein structure obtained by X-ray diffraction. A role of the water molecules displaced upon quinone binding was hypothesized, although at the present time it should be considered only as a working hypothesis.

**Acknowledgment.** The authors express their gratitude to Prof. Giovanni Venturoli for his continuous encouragement and scientific support. The MURST and CNR of Italy grants are kindly acknowledged.

## References and Notes

- (1) Feher, G.; Allen, J. P.; Okamura, M. Y.; Rees, D. C. *Nature* **1989**, *33*, 111 and references therein.
- (2) Shinkarev, V. P.; Wraight, C. A. In *The Photosynthetic Reaction Center*; Deisenhofer, J., Norris, J., Eds.; Academic Press: New York, 1993; Vol. 1, p 93.
- (3) In order to appreciate the vast amount of papers dealing with such a topic, see: *Photosynthesis: from Light to Biosphere*; Mathis, P. Ed.; Kluwer A P: The Netherlands, 1995; Vol. 1.
- (4) See for recent examples: Gunner, M. R.; Nicholls, A.; Honig, B. *J. Phys. Chem.* **1996**, *100*, 4277. Tanaka, S.; Marcus, R. A. *J. Phys. Chem. B* **1997**, *101*, 5031.
- (5) McComb, J. C.; Stein, R. R.; Wraight, C. A. *Biochim. Biophys. Acta* **1990**, *1015*, 156.
- (6) Shinkarev, V. P.; Wraight, C. A. *Biophys. J.* **1997**, *72*, 2304.
- (7) Schonfeld, M.; Montal, M.; Feher, G. *Biochemistry* **1980**, *19*, 1535.
- (8) Mallardi, A.; Palazzo, G.; Venturoli, G. *J. Phys. Chem. B* **1997**, *101*, 7850.
- (9) Warncke, K.; Gunner, M. R.; Braun, B. S.; Gu, L.; Yu, C. A.; Bruce, M.; Dutton, P. L. *Biochemistry* **1994**, *33*, 7830.
- (10) Gray, K. A.; Wachtveitl, J.; Breton, J.; Oestherheld, D. *EMBO J.* **1990**, *9*, 2061.
- (11) Okamura, M. Y.; Isaacson R. A.; Feher, G. *Proc. Natl. Acad. Sci. U.S.A.* **1975**, *72*, 3491.
- (12) Hexane molecules do not interact with the tail binding regions at the  $Q_A$  site to a degree that would cause competitive interference with binding of the ubiquinones as demonstrated by Warncke et al. in ref 9.
- (13) According to M. Straume, (*Methods Enzymol.* **1994**, *240*, 89), we indicate as "sequential" analysis the following procedure: to perform a conventional analysis relative to one of the variables and subsequently to analyze these intermediate results to account for the influence of a second variable.
- (14) Krugg, R. R.; Hunter, W. G.; Grieger, R. A. *J. Phys. Chem.* **1976**, *80*, 2335. Krugg, R. R.; Hunter, W. G.; Grieger, R. A. *J. Phys. Chem.* **1976**, *80*, 2341. Krugg, R. R.; Hunter, W. G.; Grieger, R. A. *Nature* **1976**, *261*, 566.
- (15) Chaires, J. B. *Biophys. Chem.* **1997**, *64*, 15.
- (16) Straume, M.; Johnson, M. L. *Methods Enzymol.* **1992**, *210*, 117 and references therein.
- (17) Correia, J. J.; Chaires, J. B. *Methods Enzymol.* **1994**, *240*, 593 and references therein.
- (18) The harmonic mean temperature for the experiments in LDAO aqueous solution is around 290 K as judged by Figure 5 in ref 5.
- (19) Chang, C. H.; Tiede, D. M.; Tang, J.; Smith, U.; Norris, J.; Schiffer, M. *FEBS Lett.* **1986**, *205*, 82. Allen, J. P.; Feher, G.; Yeates, T. O.; Komiya, H.; Rees, D. C. *Proc. Natl. Acad. Sci. U.S.A.* **1987**, *84*, 5730.
- (20) Ermler, U.; Fritzsche, G.; Buchanan, W.; Michel, H. *Structure* **1994**, *2*, 925.
- (21) Stowell, M. H. B.; McPhillips, T. M.; Rees, D. C.; Soltis, S. M.; Abresh, E.; Feher, G. *Science* **1997**, *276*, 812.
- (22) Jenks, W. P. *Adv. Enzymol.* **1975**, *43*, 219 and references therein.
- (23) For a recent review, see: Gilson, M. K.; Given, J. A.; Bush, B. L.; McCammon, J. A. *Biophys. J.* **1997**, *72*, 1047.
- (24) Doig, A. J.; William, D. H. *J. Am. Chem. Soc.* **1992**, *114*, 338. Searle, M. S.; Williams, D. H. *J. Am. Chem. Soc.* **1992**, *114*, 10690 and references therein.
- (25) Lancaster, C. R. D.; Michel H. *Structure* **1997**, *5*, 1339.
- (26) Larson, G. W.; Wraight, C. A. *Photosynth. Res. Suppl.* **1995**, *1*, 65.
- (27) Palazzo, G.; Giustini, M.; Mallardi, A.; Colafemmina, G.; Della Monica, M.; Ceglie, A. *Prog. Colloid Polym. Sci.* **1996**, *102*, 19.